



Impact of Diamond Nanoparticles on the Efficiency of Vinblastine against Ehrlich Solid Carcinoma in Mice

Abdulaziz M. AL-Ahmari¹ and Salim M. El-Hamidy^{1,2*}

¹*Department of Biological Sciences, Faculty of Sciences, King Abdulaziz University, Jeddah, Saudi Arabia.*

²*Princess Dr. Najla Bint Saud Al Saud Center for Excellence Research in Biotechnology, King Abdulaziz University, Jeddah, Saudi Arabia.*

Authors' contributions

This work was carried out in collaboration between both authors. Authors AMAA and SMEH designed the study, performed the statistical analysis, wrote the protocol and wrote the first draft of the manuscript. Author AMAA managed the literature searches and analyses of the study. Both authors read and approved the final manuscript.

Article Information

DOI: 10.9734/JPRI/2021/v33i20A31344

Editor(s):

(1) Dr. Giuseppe Murdaca, University of Genoa, Italy.

Reviewers:

(1) Vitor Augusto Queiroz Mauad, Brazil.

(2) M. V. Praveen Kumar, India.

Complete Peer review History: <http://www.sdiarticle4.com/review-history/67301>

Original Research Article

Received 24 January 2021

Accepted 29 March 2021

Published 02 April 2021

ABSTRACT

Aim: This investigation pointed to estimate skeletal muscle efficiency of diamond nanoparticles in enhancing Vinblastine (VBL) effects.

Methodology: One hundred Albino mice, weighing (23- 28 grams) were utilized in this research, after a week of habituation, the mice were divided into five groups at random (20 mice each). Group 1 (control) obtained distilled water infusions, Group 2 (ESC group) injected Ehrlich cells via intramuscular infusion (IM), and Group 3 (ESC+VBL group) gained Vinblastine only, Group 4 (ESC+VBL+ND) received an IM injection of Vinblastine loaded on diamond nanoparticles and Group 5 (ESC+VBL+CS+ND) received IM administration of Vinblastine stacked on Chitosan with nanodiamond. Finally, blood specimens were taken. Serum was obtained to measure Asparaginase aminotransferase, Alanine aminotransferase, and Creatinine kinase. The muscle was removed and observed under a light microscope.

*Corresponding author: E-mail: selhamidy@gmail.com;

Results: Aspartate aminotransferase (AST), alanine aminotransferase (ALT) and Creatinine kinase levels in the blood were elevated in ESC than in normal and treated groups. Levels of these enzymes were enhanced after treatment of VBL, diamond nanoparticles and chitosan.

Conclusion: Nanodiamond are influenced in the VBL delivery system for the therapy of Ehrlich Solid carcinoma in mice models. The embattled VBL liberates tumor cells and reduced the side effect of VBL on skeletal muscle.

Keywords: Cancer therapy; diamond nanoparticles; vinblastine; histopathology; skeletal muscle.

1. INTRODUCTION

The numeral applications of diamond nanoparticles in biological fields increased quickly through previous years and this imitated in huge investigations [1-3]. Several studies concentrated on pharmaceutical investigations and diagnoses of clinical applications [4].

Newly, malignancy in the whole population of the world will be the main disease due to death [5]. Cancer is many diseases that can begin when irregular cells develop irrepressibly in virtually any tissue or organ of the body, go beyond their normal borders to attack neighboring portions of the body, and/or prevail in additional organs. The final progression is called metastasizing and is the tumor's main reason for death. Additional mutual denotations for cancer are viral swelling and tumefaction [6]. With 9.6 million. Universal individuals are evaluated to have died from malignancy in 2018 [6]. Ehrlich solid melanoma is a type of homogenous neoplasia with high transplantable ability, rapid multiplication, no recrudescence, a high mortality rate, 100% tumor, and no cancer implantation antigen. It strongly matches human cancers and is frequently used as a prototype for solid tumor research [7]. This model is used to study the influence of chemical drugs on malignancy cells and to assess their responses to the host [8,9]. The identifying therapeutic method is one of its benefits, an important and valuable tool for cancer-related preclinical studies [10]. Also, it is a distinguished tool for researching and discovering antitumor activity [11]. Chemotherapy treats many types of cancer, It is very effective, but it lacks a distinction between cancer cells and healthy cells. There is various side effects are seen in patients during the chemotherapy [12]. One of the main objectives of chemotherapy is to stop the cell cycle, to stop blood vessel formation, and to stop apoptosis [13]. Hydrophobic factors characterize most types of chemotherapy, and thus the role of nanoparticles acting as chemotherapy carriers [14].

The reason for the unspecified distribution of chemotherapy to the required cells results in injury to healthy cells and tissues as well as poisoning, leading to the appearance of side effects, which is the biggest problem in cancer chemotherapy [15]. This could affect the treatment strategy, diagnosis, and treatment, and extravasation response [16]. Vinblastine is one of the most widely studied drugs in the Vinca alkaloids (Vas) family and may be part of several chemotherapy schedules for the cure of non-small cell lung melanoma, Hodgkin's lymphoma, melanoma, brain cancer, testicular cancer [17]. Breast, Leukemia, and Kaposi's Sarcoma [18]. Several alkaloids, such as vinblastine, are known as powerful chemotherapy agents in phase II clinical trials [19]. Microtubules are the first goal of several first-line drugs to treat the tumor. These medicines are considered as microtubule stabilizers such as destabilizers eribulin, and vinca alkaloids (Vinblastine), as well as have additional intricate influence [20]. Nanotechnology is the design, description, implementation, manufacturing, methods, and devices of structures by the shape and volume of the nanometer range [21]. To inspect or regulate biological procedures [22]. With completely new features and functions acquired from their 100 nm domain volume. It is used in numerous fields, including biomedicine, material development, information technology, and electronics [23], and to produce further operative treatments to progress the medical response [24]. Nanotechnology is a wide-ranging science that has the potential to help treat cancer [25]. In the latest years, nanodiamonds have attracted much attention in several fields of research, including biological sensing, medical therapy, fluorescent indicators, and enzyme immobilization [26]. NDs, particularly in cancer therapy and image sensors, are commonly used as nanomaterials for biomedical fields [27-28]. It is used as a transporter for biologically active compounds, assays and biosensors are the major purposes of NDs [29]. Serum skeletal muscle enzymes are biochemical parameters of both pathological and physiological circumstances, the functional status

of muscle tissue varies greatly. Regarding acute and chronic muscle pain, a rise in these enzymes could be a sign of cellular fibrosis or tissue injury [30]. The highest CK values are found in muscular dystrophy [31].

2. MATERIALS AND METHODS

2.1 Chemical

Detonation Diamond Nanoparticles of size around 6 nm and purity of more than 98%, Color: gray, Morphology: spherical and Bulk density: 0.17 g/cm^3 were obtained from Nanostructured & Amorphous Materials Inc., USA. Surface modified Nanodiamond contains Chitosan 15-20 wt.%. Alanine aminotransferase REF. K2143, Aspartate aminotransferase REF. K2041 and Creatinine kinase REF. K1401 was purchase from Siemens Com., Munich, Germany.

2.2 Nanodiamond Characterizations

TEM electron micrographs were occupied by JEOL-JEM 2010F electron microscope at 200KV; the specimens were discrete in 70% Ethyl alcohol and drops of nanodiamond and nanodiamond with chitosan suspensions were dried on carbon-coated copper grids. X-ray diffraction patterns were monitored by Regaku-Ultima-IV [32].

2.3 Experimental Design

In this experiment, 100 male adult Swiss mice going to weigh between 23 and 27 grams have been utilized. These animals come from King Fahd Medical Research Center (KFMRC), King Abdulaziz University, Jeddah, Saudi Arabia's animal house. Mice put in plastic enclosures (20 mice/confine) and kept in controlled lab conditions room, light: dark cycle (12:12h), temperature ($20 \pm 1^\circ\text{C}$), and moisture (65%) and fed ad libitum with the typical diet and had free drinking to tap water.

After one week of acclimation, the mice were housed in plastic enclosures (20 mice per group) and preserved in a regulated lab. They were divided into five groups at random (20 mice each). Group 1 (control) was preserved as the healthy group and was given distilled water injections Group 2 (ESC group) ESC-bearing mice were given an intramuscular injection (IM) of 0.15 ml Ehrlich cells (2×10^6), and Group 3 (ESC+VBL group) ESC-bearing mice have

infected 0.05 ml Vinblastine at a dose of 6 mg/kg. Vinblastine was given to animals via Intertumoral injection in six equal doses for two weeks, for a total dose of 6 mg/kg [33]. For about fourteen days, Group 4 (ESC+VBL+ND) received an Intertumoral infusion of 0.05 ml Vinblastine (6 mg/kg) stacked on ND nanoparticles (30 mg/kg) three times per week. Group 5 (ESC+VBL+CS+ND) received 0.05 ml Vinblastine (6 mg/kg) loaded on Chitosan with diamond nanoparticles (30 mg/kg) 3 times per week for about 2 weeks.

2.4 Blood Sampling

Blood was obtained 24 days after Ehrlich ascites carcinoma cells were injected intramuscularly [33]. Blood was drawn from the retroorbital venous plexus and placed in pure sterile test tubes with no anticoagulants. The blood specimens were centrifuged for 10 min. at 5000 rpm, and the blood sera were obtained, aliquoted, and stored at -80°C until needed [34].

2.5 Ehrlich Ascites Carcinoma Cells

King Fahd Medical Research Center, King Abdul-Aziz University, Jeddah, Saudi Arabia, generously provided the parent line of Ehrlich ascites carcinoma cells. In male albino mice, the cancer cell line was kept by serial intraperitoneal injection transplantation of Ehrlich ascites carcinoma 2.5×10^6 cancer cell cells/0.2 ml [35]. The ascitic liquid was diluted in saline solution to achieve a tumor cell suspension concentration of 10×10^6 cells/ml. 0.25 mL (2.5×10^6 cells/mice) from the inventory suspension Within 10 days, the ascetic fluid containing Ehrlich tumor cells produced and was gathered via i.p. puncture with a sterile syringe, dilution, and including the cells via a Neubauer Hemocytometer [36]. Ehrlich cells were intramuscular injection (IM) to get the solid tumor.

2.6 Histopathological Examination

Muscle tissues in various groups and fixed in 10% formal saline for 24 hrs. After sterilizing the water, various concentrations of ethyl alcohol were used to dehydrate the samples. Specimens were cleared in xylene and embedded in paraffin for twenty-four hours at 56 degrees in a hot air oven. By microtome, paraffin blocks were prepared for sectioning at a thickness of 4 microns. For the investigation, the acquired tissue sections were placed on glass

slides, deparaffinized, and stained with hematoxylin and eosin stains. Finally, using a light microscope (Olympus BX 51, Olympus America, Melville, NY) and a digital camera, an examination was performed at different magnification [37].

2.7 Blood Biochemical Parameters

2.7.1 Aspartate aminotransferase (AST)

The aspartate aminotransferase procedure was evaluated using a bichromatic (340-700 nm) rate method, which is a modification of the technique established by the International Federation of Clinical Chemistry (IFCC) [38].

2.7.2 Alanine aminotransferase (ALT)

The Alanine Aminotransferase (ALT) method used by Dimension Vista is an evolution of the IFCC's suggested ALT protocol as mentioned by [39]. A bichromatic (340, 700 nm) rate method is used to measure the alteration in the absorption spectrum, which is directly related to ALT levels [39].

2.7.3 Creatine Kinase (CK)

The Dimension Vista CK technique is enhanced to usages the International Federation of Clinical Chemistry (IFCC) CK 37°C [40].

3. RESULTS

3.1 Nanodiamond Characterization

3.1.1 TEM examination

Fig. 1 reveals the TEM images for the diamond nanoparticles before and after functionalization with chitosan. It is noticed that the diamond nanoparticle before functionalization showed individual nanoparticles with a mean size of 7 ± 2 nm. After functionalization with chitosan, the diamond nanoparticles tend to aggregate and form large particles, where the mean size of the diamond reached 10 ± 1 nm. The high-resolution TEM images before and after functionalization showed a slight increase of the d-space parameter, where it is increased from 0.52 nm to 0.56 nm.

3.1.2 XRD

Fig. 2 represents the XRD for the diamond nanoparticles before and after functionalization with chitosan. It is noticed that the two strong peaks located at 2θ values of 43.2° and 74.6° were assigned to the reflections from (1 1 1) and (2 2 0) plane of the diamond. The broad peak appeared at 2θ value of 20.1° was ascribed to the amorphous carbon. The intensity of this peak is increased due to the functionalization of the surface of diamond nanoparticles with chitosan.

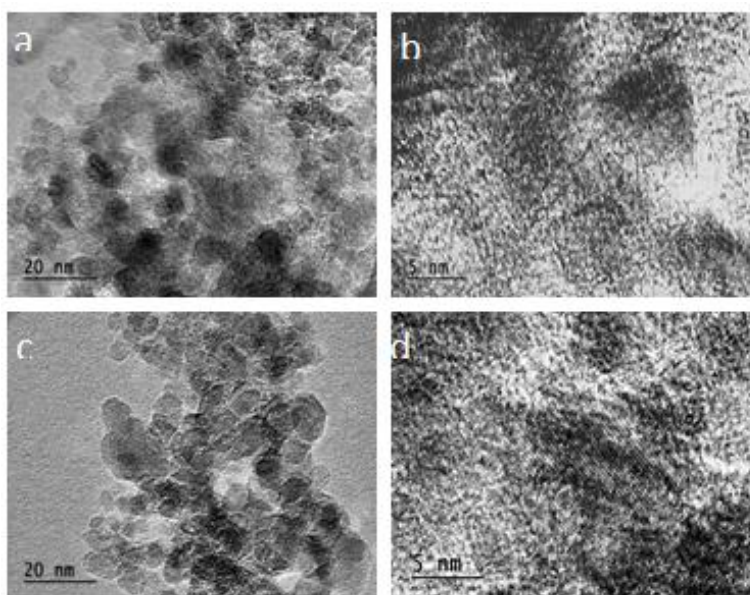


Fig. 1. a, b electron micrograph of diamond nanoparticles and c, d diamond nanoparticles with chitosan (scale bar a, c: 20 nm and b, d: 5 nm)

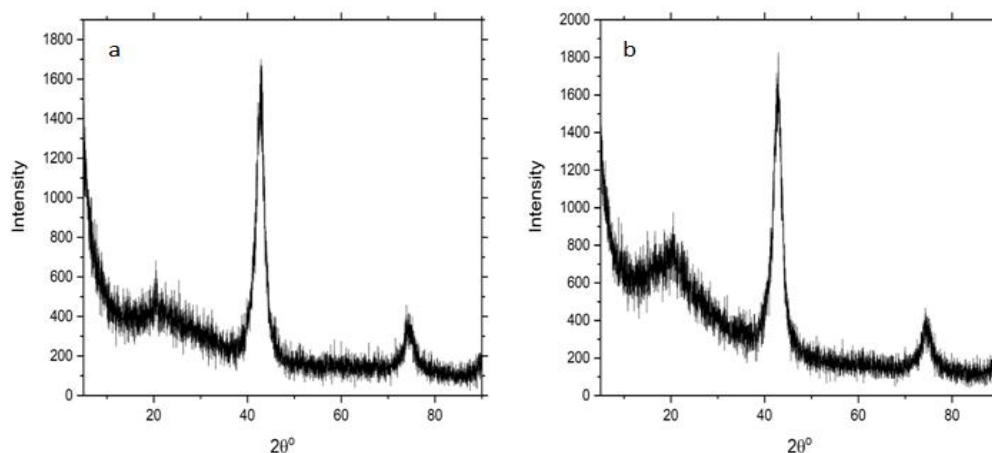


Fig. 2. a. X-ray diffraction pattern of diamond Nanoparticles b. X-ray diffraction pattern of diamond nanoparticles-chitosan

3.2 Histopathological Examination

Light microscope images of longitudinal and cross-sections of the mice back thigh muscle: (A-D); Control, (E-H); Ehrlich solid carcinoma, (I-L); Ehrlich solid carcinoma treated by Vinblastine, (M-P); Ehrlich solid carcinoma treated with Vinblastine and Nanodiamond, (Q-T); Ehrlich solid carcinoma treated with Vinblastine and Nanodiamond NPs and Chitosan. (M) musculoskeletal fibroblasts, (K) sarcoplasm between fibers, (N) Necrosis, Cancer cells (yellow arrows), and Muscle cell nucleus (White arrows).

Micrograph of the skeletal muscles of Control group mice (A-D); It shows the normal cells and tissue shape of the muscles, (M) musculoskeletal fibroblasts, (K) sarcoplasm between fibers, Muscle cell nucleus (White arrows), (A-B) Longitudinal muscles, (C-D) Transverse muscles, (A-C 100X) (B-D 400X). Micrograph of the skeletal muscles of Ehrlich group mice (E-F) extensive infiltration of the muscle tissue with tumor cells generally, A. aggregation of cancer cells (yellow arrows), (N) Extensive necrosis and fibrosis, (M) musculoskeletal fibroblasts, (K) sarcoplasm between fibers, (E-F) Longitudinal muscles, (G-H) Transverse muscles, (E-G 100X) (F-H 400X). Micrograph of the skeletal muscles of Ehrlich+Vinblastine group mice (I-L), In general, there was an improvement in tissue and cells after using vinblastine and a reduction in cancer cells compared to the previous group, (N) Extensive necrosis and fibrosis, (M) musculoskeletal fibroblasts, (K) sarcoplasm between fibers, Muscle cell nucleus (White

arrows), (I-J) Longitudinal muscles, (K-L) Transverse muscles, (I-K 100X) (J-L 400X). Micrograph of the skeletal muscles of Ehrlich+Vinblastine+Nanodiamond group mice (M-P), There is an enhancement in cells and tissue and moderate of cancer and inflammatory cells compared to the Ehrlich + Vinblastine group, (N) moderate necrosis and fibrosis, (M) musculoskeletal fibroblasts, (K) sarcoplasm between fibers, Muscle cell nucleus (White arrows), (M-N) Longitudinal muscles, (O-P) Transverse muscles, (M-P 100X) (O-N 400X). Micrograph of the skeletal muscles of Ehrlich+Vinblastine+Nanodiamond+Chitosan group mice (Q-T), There is perfection in muscle tissue and cells. Also, an important clear reduction of cancer cells, (M) musculoskeletal fibroblasts, (K) sarcoplasm between fibers, Muscle cell nucleus (White arrows), (Q-R) Longitudinal muscles, (S-T) Transverse muscles, (Q-S 100X) (R-T 400X).

3.3 Blood Biochemical Parameters

Serum levels of ALT and AST were significantly increased in ESC, ESC+VB, ESC+VB+ND, and ESC+VB+ND-CS groups versus the control group. ALT, AST, and Creatinine kinase levels were significantly decreased in ESC+VB, ESC+VB+ND, and ESC+VB+ND-CS groups versus ESC group ($P < 0.0001$ for all); in ESC+VB+ND and ESC+VB+ND-CS groups versus ESC+VB group ($P < 0.0001$). In ESC+VB+ND-CS group, AST and ALP were significantly increased versus ESC+VB+ND group (Table 1 and Fig. 4).

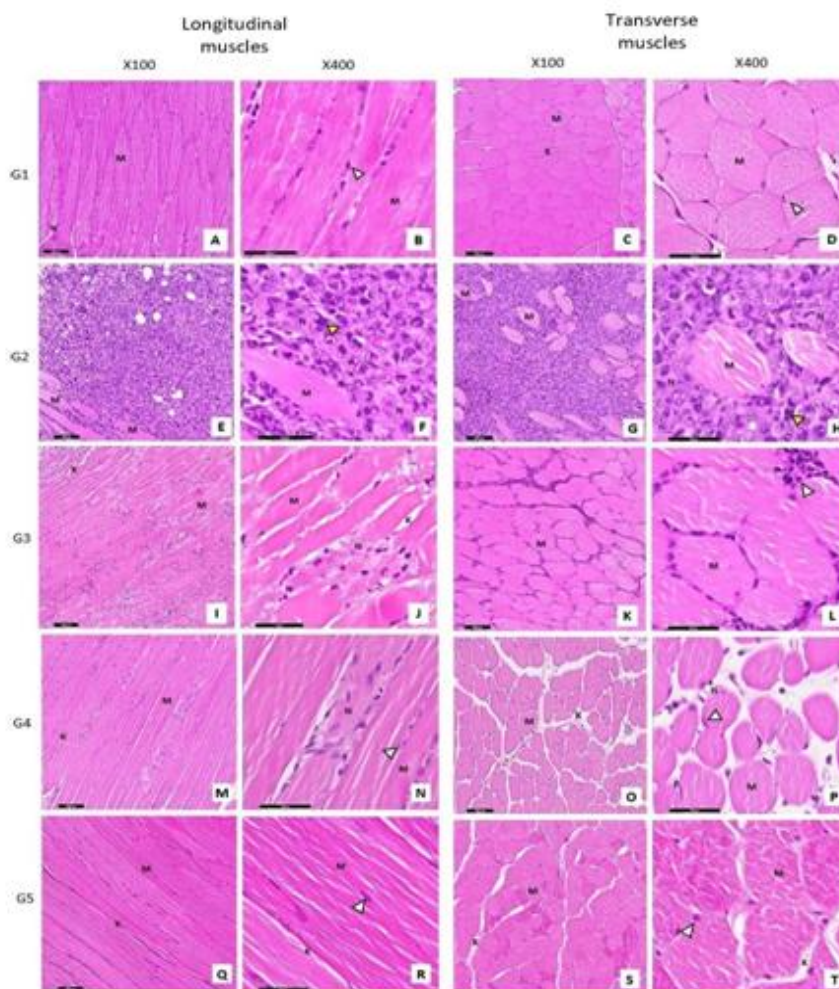


Fig. 3. Light Photographs of histological sections from mice skeletal muscle at various magnifications X100 & X400 to show (G1- G2 - G3- G4 - G5) stained by H&E

Table 1. Comparison of Aspartate aminotransferase and Alanine aminotransferase in different studied groups

Groups Parameters	Control	ESC	ESC+VB	ESC+VB+ND	ESC+VB+ND-CS
AST (U/L)	21.25±0.25	201.53±0.55	39.25±0.25	17.25±0.25	20.17±0.14
Significance	-	¹ P =0.0001	¹ P=0.0001; ² P=0.0001	¹ P=0.0001; ² P=0.0001, ³ P=0.0001	¹ P=0.002; ² P=0.0001, ³ P=0.0001; ⁴ P=0.0001
ALT (U/L)	17.17±0.14	190.25±0.25	31.25±0.25	13.50±0.25	13.08±0.14
Significance	-	¹ P =0.0001	¹ P=0.0001; ² P=0.0001	¹ P=0.0001; ² P=0.0001, ³ P=0.0001	¹ P=0.0001; ² P=0.0001, ³ P=0.0001; ⁴ P=0.038

Data were expressed as mean +/- standard deviation. ¹P: Significant change compared to the control group; ²P: Significant change compared to the Ehrlich group (ESC) group; ³P: Significant change compared to the Ehrlich and Vinblastine group (ESC+VB) group; ⁴P: Significant change compared to the Ehrlich, Vinblastine, and Nanodiamond group (ESC+VB+ND) group. Significance was made using ANOVA-oway test at P = 0.05

Serum levels of creatinine kinase were significantly increased in ESC, ESC+VB, ESC+VB+ND and ESC+VB+ND versus the control group ($P < 0.0001$ for all) and in ESC+VB+ND-CS group versus ESC+VB+ND group ($P < 0.0001$). Creatinine kinase levels were

significantly decreased in ESC+VB, ESC+VB+ND, and ESC+VB+ND-CS groups versus ESC group ($P < 0.0001$ for all); in ESC+VB+ND versus ESC+VB ($P < 0.0001$) (Table 2 and Fig. 5).

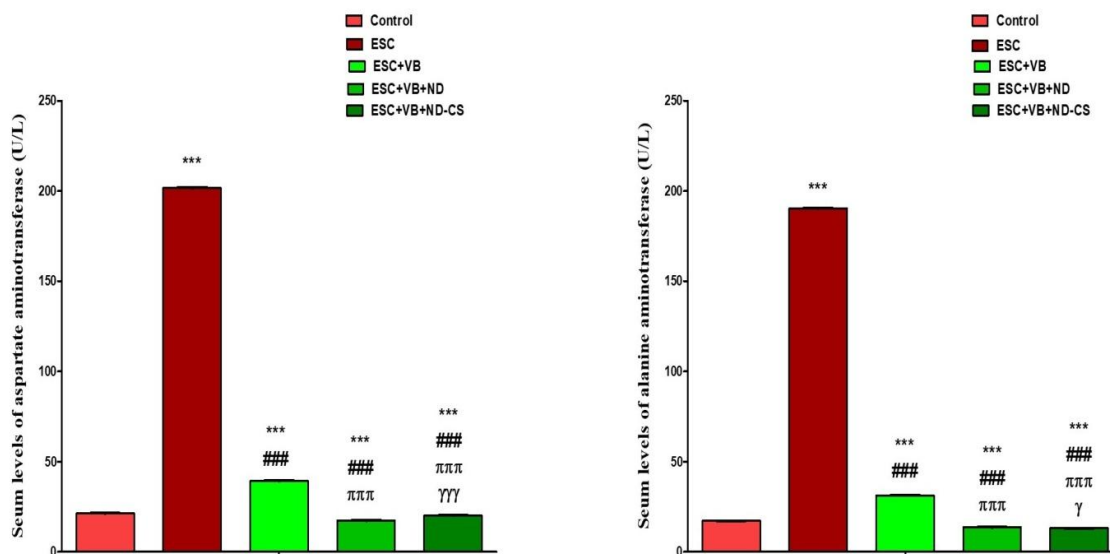


Fig. 4. Comparison of serum levels of alanine aminotransferase and aspartate aminotransferase in different studied groups

*: Significant change compared to the control group; #: Significant change compared to the Ehrlich Solid Carcinoma (ESC) group; π: Significant change compared to the Ehrlich Solid Carcinoma and VB (ESC+VB) group; γ: Significant change compared to the Ehrlich Solid Carcinoma +VB+ND (ESC+VB+ND) group

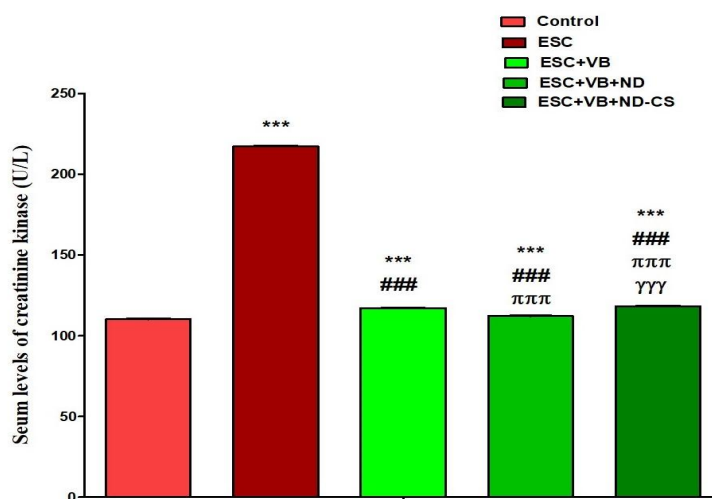


Fig. 5. Comparison of serum levels of creatinine kinase in different studied groups

*: Significant change compared to the control group; #: Significant change compared to the Ehrlich Solid Carcinoma (ESC) group; π: Significant change compared to the Ehrlich Solid Carcinoma and VB (ESC+VB) group; γ: Significant change compared to the Ehrlich Solid Carcinoma +VB+ND (ESC+VB+ND) group

Table 2. Comparison of creatinine kinase in different studied groups

Groups Parameters	Control	ESC	ESC+VB	ESC+VB+ND	ESC+VB+ND-CS
Creatinine kinase (U/L)	110.23±0.25	217.25±0.25	117.20±0.17	112.18±0.16	118.23±0.21
Significance	-	¹ P =0.0001	¹ P=0.0001; ² P=0.0001	¹ P=0.0001; ² P=0.0001, ³ P=0.0001	¹ P=0.0001; ² P=0.0001, ³ P=0.0001; ⁴ P=0.0001

Data were expressed as mean +/- standard deviation. ¹P: Significant change compared to the control group; ²P: Significant change compared to the Ehrlich group (ESC) group; ³P: Significant change compared to the Ehrlich and Vinblastine group (ESC+VB) group; ⁴P: Significant change compared to the Ehrlich, Vinblastine, and Nanodiamond group (ESC+VB+ND) group. Significance was made using ANOVA-one way test at P = 0.05

Table 3. Comparison of oxidative stress markers between different studied groups

Groups Parameters	Control	ESC	ESC+VB	ESC+VB+ND	ESC+VB+ND-CS
SOD (U/ml)	177.15±0.13	98.40±0.36	100.20±0.18	167.13±0.12	160.18±0.18
Significance	-	¹ P =0.0001	¹ P=0.0001; ² P=0.0001	¹ P=0.0001; ² P=0.0001, ³ P=0.0001	¹ P=0.0001; ² P=0.0001, ³ P=0.0001; ⁴ P=0.001
GSH (ng/ml)	14.57±0.06	2.07±0.06	10.12±0.13	14.10±0.10	13.37±0.06
Significance	-	¹ P =0.0001	¹ P=0.0001; ² P=0.0001	¹ P=0.0001; ² P=0.0001, ³ P=0.0001	¹ P=0.0001; ² P=0.0001, ³ P=0.0001; ⁴ P=0.0001
CAT (Mu/L)	111.25±0.25	51.13±0.15	99.33±0.38	109.42±0.38	100.17±0.15
Significance	-	¹ P =0.0001	¹ P=0.0001; ² P=0.0001	¹ P=0.0001; ² P=0.0001, ³ P=0.0001	¹ P=0.0001; ² P=0.0001, ³ P=0.005; ⁴ P=0.0001
MDA (nmol/ml)	0.33±0.01	1.90±0.01	1.11±0.01	0.95±0.01	1.00±0.01
Significance	-	¹ P =0.0001	¹ P=0.0001; ² P=0.0001	¹ P=0.0001; ² P=0.0001, ³ P=0.0001	¹ P=0.0001; ² P=0.0001, ³ P=0.0001; ⁴ P=0.0001

Data were expressed as mean +/- standard deviation. ¹P: Significant change compared to the control group; ²P: Significant change compared to the Ehrlich group (ESC) group; ³P: Significant change compared to the Ehrlich and Asparaginase group (ESC+VB) group; ⁴P: Significant change compared to the Ehrlich, Asparaginase, and Halloysite nanotubes group (ESC+VB+ND) group. Significance was made using ANOVA-one way test at P = 0.05. SOD: superoxide dismutase; GSH: glutathione; MDA: malondialdehyde; CAT: catalase

SOD serum levels were significantly decreased in ESC, ESC+VB, ESC+VB+ND, and ESC+VB+ND-CS groups versus the control group ($P < 0.0001$ for all). SOD levels were significantly increased in ESC+VB, ESC+VB+ND and ESC+VB+ND-Cs groups versus ESC group ($P < 0.0001$ for all); and in ESC+VB+ND-CS group versus ESC+VB+ND group ($P < 0.0001$ and $P = 0.001$), in ESC+VB+ND and ESC+VB+ND-CS groups versus ESC+VB group ($P < 0.0001$ both) and in ESC+VB+ND-CS

versus ESC+VB+ND ($P < 0.0001$). GSH and CAT serum levels were significantly decreased in ESC, ESC+VB, ESC+VB+ND, and ESC+VB+ND-CS groups versus the control group ($P < 0.0001$ for all) and in and in ESC+VB+ND-CS versus ESC+VB+ND ($P < 0.0001$). GSH and CAT levels were significantly increased in ESC+VB, ESC+VB+ND, and ESC+VB+ND-Cs groups versus ESC group ($P < 0.0001$ for all); and in ESC+VB+ND-CS group versus ESC+VB+ND

group, in ESC+VB+ND and ESC+VB+ND-CS groups versus ESC+VB group. MDA serum levels were significantly increased in ESC, ESC+VB, ESC+VB+ND, and ESC+VB+ND-CS groups versus the control group ($P < 0.0001$ and $P = 0.008$) and in ESC+VB+ND-CS versus ESC+VB+ND ($P < 0.0001$). MDA levels were

significantly decreased in ESC+VB, ESC+VB+ND, and ESC+VB+ND-Cs groups versus ESC group ($P < 0.0001$ for all); in ESC+VB+ND and ESC+VB+ND-CS groups versus ESC+VB group ($P < 0.0001$ for both) (Table 3 and Fig. 6).

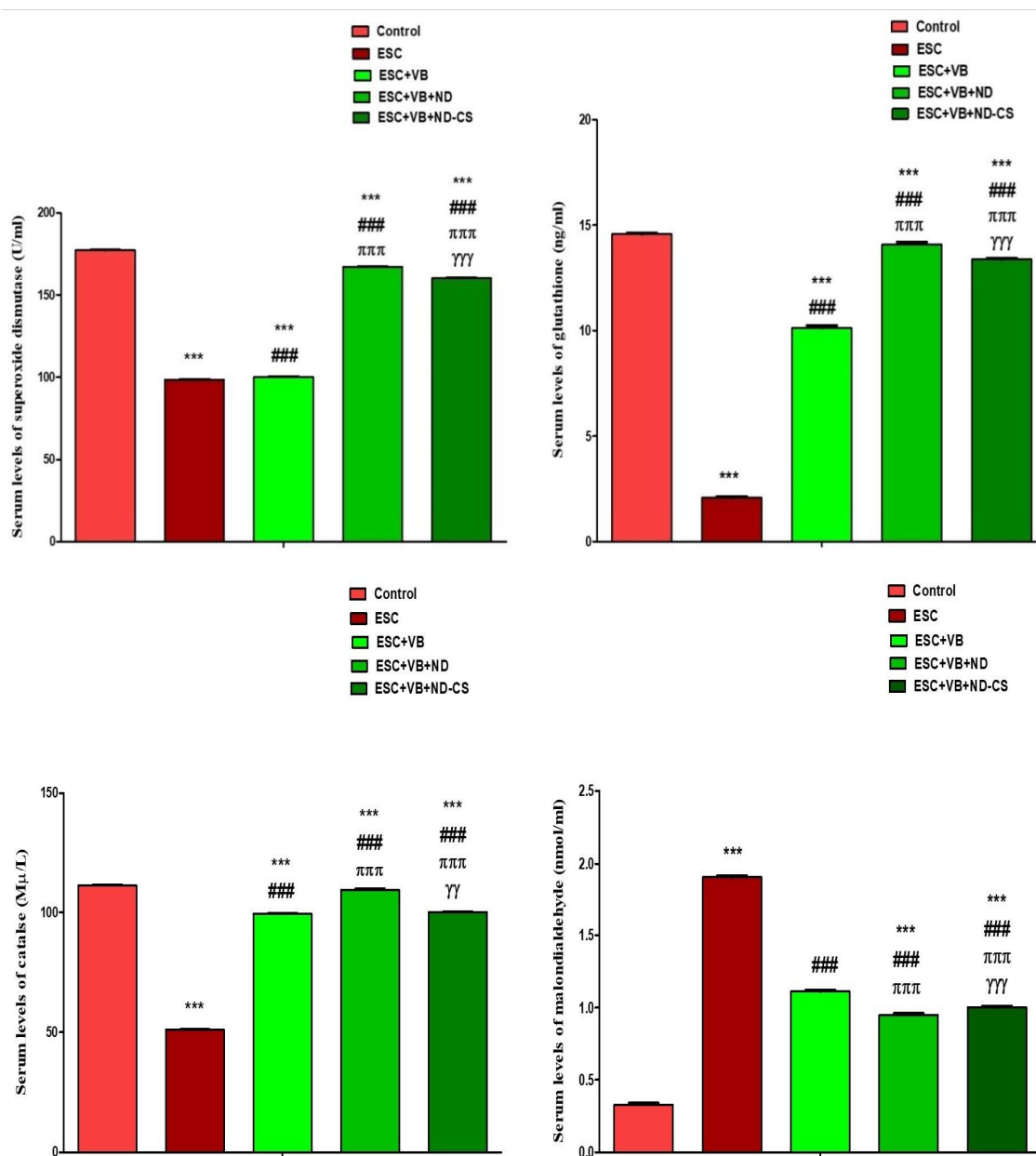


Fig. 6. Comparison of serum levels of malondialdehyde in different studied groups
 †: Significant change compared to the control group; #: Significant change compared to the Ehrlich Solid Carcinoma (ESC) group; π: Significant change compared to the Ehrlich Solid Carcinoma and VB (ESC+VB) group; γ: Significant change compared to the Ehrlich Solid Carcinoma +VB+ND (ESC+VB+ND) group

4. DISCUSSION

Cancer is a highly congregation and varied gathering of diseases marked through unrestricted cell generation, attack of limited tissues, and distant metastases [40]. The cancer models have the benefit of little price, easy reproducibility, and accessibility are that transplantable [41].

Ehrlich ascites carcinoma (EAC) is an unformed sarcoma caused by high prevalence, increased ability to the implant, and a high mortality rate [7]. EAC is similar to human carcinoma, so the ascetic and solid forms of this carcinoma are often used to assess the anticancer efficiency of various cancers [42].

Ehrlich's melanoma has powerful inflammatory occurrences, such as ischemia and inflammatory infects, which are assumed to perform a significant role in cancer development in several kinds of malignancy [43].

The main carcinoma cell variant of Ehrlich ascites is glioma mammary adenocarcinoma [43]. A large proportion of techniques used during cancer treatment are chemotherapy, which kills cancer cells by induction of apoptosis and has a significant effect on patients' lifestyles, and is a clear cause of mortality [44].

By enhancing the bioavailability and therapeutics of anti-cancer drugs, nanotechnology has been used to improve cancer treatment. The utilize of nanotechnology in cancer treatment provides inspiring opportunities, composes the potential for new targeted drug delivery systems to abolish cancers with negligible injury to healthful tissue. Interactions with nanoparticle cells are very reliant on particle shape, dimensions, and charge [45]. For cellular endocytosis, the optimum particle diameter is 25-30 nm [46]. The primary constituents for bionanocomposite preparation are polymers of biological origin, including the increasing application of chitosan, a natural polysaccharide [47].

The alkaloid derivative from the periwinkle plant is vinblastine. It prevents cell division by interfering with the mitotic spindle. Inhibition of the formation of microtubules in the mitotic spindle has been linked to the mode of action of vinblastine resulting throughout the arrest of cell division at the metaphase stage.

The outcomes of the current investigation showed that serum creatinine kinase concentrations were significantly greater than those of the normal group after injection of the Ehrlich cells of albino mice. While only CK activities were significantly reduced compared to the ESC group of mice after vinblastine treatment of Ehrlich solid Carcinoma mice. Meanwhile, creatinine kinase levels were significantly reduced compared with tumor mice after vinblastine and CS-ND NPs treatment. The level of creatinine kinase is almost like the control group's level. These outcomes were consistent with Alkhatib et al. [48] that an increase in EAC-bearing mice creatinine kinase (CK) levels was comparable to the control group.

AST, ALT, and CK have been used for liver and skeletal injury recognition in therapeutic applications. As ALT and AST are indeed explained in other body tissue (skeletal muscle, for example), tissue damage may be under-or-over in the apparent lack of further liver-specific assays [49].

Serum concentrations of muscle enzymatic are in pathogenesis situations, parameters of the cognitive function of muscle and differ greatly. Creatine kinase, lactate dehydrogenase, and aspartate aminotransferase are the utmost efficient serum indicators of muscle damage, but autophagy in skeletal muscles may be affected by chronic inflammation following intensive activity. Therefore, some identifiers, like superoxide dismutase, glutathione, catalase, and malondialdehyde, are used to evaluate the level of muscle stress [50].

Creatinine kinase (CK) and lactate dehydrogenase (LDH) are physiological biomarkers for cell necrosis and acute or chronic muscle atrophy. CK and LDH activation may rise symptoms like pain, fatigue, and a decrease in muscle strength due to damaged skeletal muscles during high-intensity long-distance exercise [51]. The physiological identifiers for cellular proliferation and acute or chronic muscle damage are Creatinine Kinase (CK) and lactate dehydrogenase (LDH). Expression of CK and LDH will enhance chronic pain, nausea, and loss of muscle mass during high-impact deep activity damaged muscle tissue [51].

Retinol enzymatic assessments have been utilized in a wide range of implementation in the hospital [52]. The variation of serum enzymes, including CK, ALT, and AST, have been

expected to enhance muscle dystrophy [53]. The elevated serum enzymes in dystrophinopathy are largely attributed to their uptake from damaged muscle fibers rather than liver damage, as demonstrated by liver biopsy in patients [54]. The altitude of CK and aminotransferase rates in dystrophinopathy is easy to comprehend because of the tissue dispersion of enzymes: ALT and AST are indeed allocated in the liver and muscles, while CK is strongly allocated in the muscles [55]. Even though aminotransferases are commonly used in treatment centers as responsive biological markers for hepatocyte injury, in certain cases, the contest among elevated serum CK and dystrophinopathy aminotransferases are reflective of muscle injury.

Some studies have shown that by raising the level of oxygen radicals in cancer cells or going to target the nucleus or many other tissue cells, several chemically altered nanoparticles can destroy cancer cells [56-58].

In this study, a strong correlation was observed between alterations in antioxidant mechanisms, angiogenesis, and Ehrlich solid tumor cell proliferation. A significant statistically elevated level of MDA and reduced level of SOD, GSH, and Catalase occurred in tissues obtained from the cancer group. nanodiamond can modify antioxidative enzyme operation by sponsoring the amounts of SOD, GSH, and Catalase, in addition to preventing the rate of MDA. These findings coincide with many other studies finding high levels of MDA in breast cancer.

The results here are harmonious with those of Abd El-Aziz et al. [59]. Ehrlich tumors have been observed to show substantial increases in MDA and substantial reductions in catalase and SOD catalase. Moselhi and Al Mslmani [60], suggest that decreased levels of SOD could lead to the changed antioxidant activity instituted by angiogenesis. Oxidative stress-induced by increased production of free radicals, which can elicit oxidative damage in vivo, damages molecules such as fats [61]. The decreased expression of GSH observed in cancer mice could be due to the rise in the level of conversion of GSH to oxidized GSH to reduce the hydrogen peroxide intracellular level.

The most utilized cancer cells are highly irrelevant and have a fast growth rate that makes them extremely responsive to cancer treatment as well [7]. Excessive production of ROS causes oxidative cellular injury to macromolecules, and

even DNA, leading to many types of oxidative stress, such as with single base and sugar-phosphate destruction [62].

The results obtained from the figures and tables show that in the case of MDA levels proportional to healthy mice, the ESC group was very high, but the VBL+ND-CS treated groups improved MDA. Dissimilar to the GSH, SOD, and catalase liver that were lower than the healthy mice and treated groups, the antioxidant content of the liver was significantly increased. Indeed, the growth and invasion of tumor cells cause disturbances in antioxidant processes by generating high amounts of free radicals, which can contribute to mutating and damaging normal tissues. There is a strong correlation between alterations in metabolic processes and tumor cell proliferation [63]. Glutathione redox decreased significantly increased oxidative stress through tumor growth in Ehrlich ascites, causing an increase in GSSG rates [64]. SOD and CAT are key enzymes that play a major role in tumorigenesis during oxidative stress, leading to the deterioration of ROS scrounging enzymes when the antioxidants are restricted or inhibited [65]. AuNP therapy has been shown to improve the capability of the liver and kidneys and decrease oxidation stress by rising antioxidant variables, based on the obtained results [66].

Pro-oxidant chemicals that excite the potential of oxidation either by synthesis or by inhibiting antioxidants can cause cell and tissue injury [67], due to the formation of superoxidation, leading to the rupture of the plasma membrane and organelles [68]. Among the main causes of nearly degenerative diseases are reactive oxygen species. The antioxidant protection ability is overwhelmed by oxidative stress-induced when ROS and free radicals are generated [69]. By increasing the levels of endogenous antioxidants in the body and thus reducing the process of lipid peroxidation, antioxidants have protective and therapeutic values against different diseases [70]. In turn, lipid peroxidation is seen as an indicator of structural and functional alterations of cellular and organelle membranes with failure to stop the formation of extreme free radicals by cellular oxidative [71].

5. CONCLUSION

The current study aims to be effective in lowering the risk of cancer complications. Furthermore, the use of diamond nanoparticle drug delivery can recognize several important drug delivery

challenges. After therapy with vinblastine and ND-CS, the concentrations of AST, ALT, and CK enzymes are similar to the control group. In mice models, nanodiamond is influenced in the VB delivery system for the treatment of Ehrlich Solid Carcinoma. The beleaguered VB liberates tumor cells and decreases VB's skeletal muscle side effects.

CONSENT

It is not applicable.

ETHICAL APPROVAL

All research stages were performed following Canadian Ethical Standards for the use of trial animals. The Rural Biomedical Ethical Committee of King Abdulaziz University in Jeddah, Saudi Arabia, approved the evaluation configuration.

ACKNOWLEDGEMENT

I would like to express my gratitude to King Abdulaziz University, Faculty of Sciences, Biological Sciences Department, for allowing us to study and allocating laboratories and private spaces to us.

COMPETING INTERESTS

Authors have declared that no competing interests exist.

REFERENCES

1. Torelli MD, Nunn NA, Shenderova OAA. Perspective on Fluorescent Nanodiamond Bioimaging. *Small*. 2019;15(48):1902151.
2. Shenderova OA, Shames AI, Nunn NA, et al. Review article: synthesis, properties, and applications of fluorescent diamond particles. *J Vac Sci Technol B*. 2019;37(3): 030802.
3. Jariwala DH, Patel D, Wairkar S. Surface functionalization of nanodiamonds for biomedical applications. *Mater Sci Eng C*. 2020;113:110996.
4. Chauhan S, Jain N, Nagaich U. Nanodiamonds with powerful ability for drug delivery and biomedical applications: recent updates on in vivo study and patents. *J Pharm Anal*. 2020;10(1):1–12.
5. Bray F, Ferlay J, Soerjomataram I, Siegel RL, Torre LA, Jemal A. Global cancer statistics 2018: GLOBOCAN estimates of incidence and mortality worldwide for 36 cancers in 185 countries. *CA: A Cancer Journal for Clinicians*. 2018;68(6):394-424. Available: https://www.who.int/health-topics/cancer#tab=tab_1
6. Ozaslan M, Karagoz ID, Kilic IH, Guldur ME. Ehrlich ascites carcinoma. *Afr J Biotechnol*. 2011;10(13): 2375-2378.
7. Campos CC, Zarpelon AC, Correa M, Cardoso RD, Pinho-Ribeiro FA, Cecchini R, et al. The Ehrlich tumor induces pain-like behavior in mice: A novel model of cancer pain for pathophysiological studies and pharmacological screening. *Biomed. Res. Int*. 2013;624815:1-12.
8. Ali BM, Zaitone SA, Shouman SA, Moustafa YM. Dorzolamide synergizes the antitumor activity of mitomycin C against Ehrlich's carcinoma grown in mice: role of thioredoxin-interacting protein. *Naunyn Schmiedeberg's Arch. Pharmacol*. 2015; 388(12):1271-1282.
9. Frajacom FTT, de Souza Padilha, C, Marinello PC, Guarnier FA, Cecchini R, Duarte JAR, Deminice R. Solid Ehrlich carcinoma reproduces functional and biological characteristics of cancer cachexia. *Life Sciences*. 2016;162:47-53.
10. Gaballah HH, Gaber RA, Mohamed DA. Apigenin potentiates the antitumor activity of 5-FU on solid Ehrlich carcinoma: Crosstalk between apoptotic and JNK-mediated autophagic cell death platforms. *Toxicology and Applied Pharmacology*. 2017;316:27–35.
11. Barreto JA, O'Malley WO, Kubeil M, Graham B, Stephan H, Spiccia L. Applications in cancer imaging and therapy Nanomaterials. *Advanced materials Mater*. 2011;23(12):18-40.
12. Hassan M, Watari H, AbuAlmaaty A, Ohba Y, Sakuragi N. Apoptosis and molecular targeting therapy in cancer. *Biomed Res Int*. 2014;150845.
13. Sun T, Zhang YS, Pang B, Hyun DC, Yang M, Xia Y. Engineered nanoparticles for drug delivery in cancer therapy. *Angewandte Chemie International Edition*. 2014;53(46):12320-12364.
14. Nair LK, Jagadeeshan S, Nair SA, Kumar GSV. Biological evaluation of 5- fluorouracil nanoparticles for cancer chemotherapy and its dependence on the carrier. *PLGA, Int. J. Nanomed*. 2011;6:1685-1697.
15. Robinson A, Souied O, Bota AB, Levasseur N, Stober C, Hilton J, et al. Optimal vascular access strategies for patients receiving chemotherapy for early-stage

- breast cancer: a systematic review. *Breast Canc Res Treat.* 2018;171(3):607-620.
17. Moudi MA, Go RU, Yong SYCH, Nazre MO. Vinca alkaloids. *Int J Prev Med.* 2013; 4(11):1231-5.
 18. Cragg GM, Newman DJ. Plants as a source of anti-cancer agents. *J Ethnopharmacol.* 2005;100(1-2):72-79.
 19. Yardley DA, McCleod M, Schreiber F, Murphy P, Patton J, Thompson DS, et al. A phase II trial of vinflunine as monotherapy or in combination with trastuzumab as first-line treatment of metastatic breast cancer. *Canc. Invest.* 2010;28(9):925-31.
 20. Yang W, Peters JI, Williams RO. Inhaled nanoparticles- a current review. *Int J Pharm.* 2008;356(1-2):239-247.
 21. Fakruddin M, Hossain Z, Afroz H. Prospects and applications of nanobiotechnology: A medical perspective. *J Nanobiotechnol.* 2012;10(40):1-8.
 22. Kim ES, Ahn EH, Chung E, Kim DH. Recent advances in nanobiotechnology and high-throughput molecular techniques for systems biomedicine. *Mol Cells.* 2013; 36(6):477-484.
 23. Ren Y, Zhang H, Chen B, Cheng J, Cai X, Liu R, et al. Multifunctional magnetic Fe₃O₄ nanoparticles combined with chemotherapy and hyperthermia to overcome multidrug resistance. *Int J Nanomed.* 2012;7:2261-2269.
 24. Huang CY, Ju DT, Chang CF, Muralidhar RP, Velmurugan BK. A review on the effects of current chemotherapy drugs and natural agents in treating non-small cell lung cancer. *BioMedicine.* 2017;7(4): 12-23.
 25. Sengupta S, Eavarone D, Capila I, Zhao G, Watson N, Kiziltepe T, Sasisekharan R. Temporal targeting of tumour cells and neovasculature with a nanoscale delivery system. *Nature.* 2005;436(7050):568-72.
 26. Zhang Y, Chan HF, Leong KW. Advanced materials and processing for drug delivery: the past and the future. *Adv. Drug Delivery Rev.* 2013;65(1):104-20.
 27. Martel-Estrada S. Recent Progress in Biomedical Applications of Nanodiamonds. *Nanoscience and Nanotechnology.* 2018; 8(1):11-24.
 28. Ansari SA, Satar R, Zaidi SK, Naseer MI, Karim S, Alqahtani MH, Rasool M. Nanodiamonds as an effective and novel matrix for immobilizing β galactosidase. *Food and Bioproducts Processing.* 2015; 95:298-303.
 29. Mytych J, Lewinska A, Zebrowski J, Wnuk M. Nanodiamond-induced increase in ROS and RNS levels activates NF- κ B and augments thiol pools in human hepatocytes. *Diamond and Related Materials.* 2015;(55):95-101.
 30. Wu MS, Sun DS, Lin YC, Cheng CL, Hung SC, Chen PK, et al. Nanodiamonds protect skin from ultraviolet B-induced damage in mice. *J Nanobiotechnology.* 2015;(7):13 35.
 31. Cervellini G, Comelli I, Lippi G. Rhabdomyolysis: Historical background, clinical, diagnostic and therapeutic features. *Clin Chem Lab Med.* 2010;48(6): 749-756.
 32. El-Bohy AA, Wong BL. The diagnosis of muscular dystrophy. *Pediatr Ann.* 2005; 34(7):525-30.
 33. Shukla G, Aiyer H. Thermal Conductivity Enhancement of Transformer Oil using Functionalized Nanodiamonds. *IEEE Transactions on Dielectrics and Electrical Insulation.* 2015;22(4):2185-2190.
 34. Salem FS, Badr M, Neamat-Allah A. Biochemical and pathological studies on the effects of levamisole and chlorambucil on Ehrlich ascites carcinoma-bearing mice. *Vet Ital.* 2011;47(1):89-95.
 35. Hoff J. Methods of Blood Collection in the Mouse. *Lab Animal.* 2000;29(10):47-53.
 36. Gothoskar SV, Ranadive KJ. Anticancer screening of SAN-AB; An extract of marking nut, *Semecarpus anacardium*. *Indian J Exp Bio.* 1971;9(3):372-375.
 37. Khedr NF, Khalil RM. Effect of hesperidin on mice bearing Ehrlich solid carcinoma maintained on doxorubicin. *Tumor Biol.* 2015;36(12):9267–9275.
 38. Wang J, Wang L, Long L, et al. Solitary renal metastasis from squamous cell carcinoma of the lung: A case report. *Medicine (Baltimore).* 2019;98(5):e14310.
 39. Tietz F, Haanappel V, Mai A, Mertens J, Stöver D. Performance of LSCF cathodes in cell tests. *Journal of Power Sources.* 2006;156(1):20-22.
 40. Bergmeyer H, Scheibe P, Wahlefeld A. Optimization of methods for aspartate aminotransferase and alanine aminotransferase. *Clinical chemistry.* 1978;24:58-73.
 41. Wroblewski F, Ladue JS. Serum glutamic pyruvic transaminase in cardiac and hepatic disease. *Proceedings of the*

- Society for Experimental Biology and Medicine. 1956;91(4):569-571.
42. Siekmann L, Bonora R, Burtis CA, Ceriotti F, Clerc-Renaud P, Féraud G, Hoelzel W. International Federation of Clinical Chemistry and Laboratory Medicine. IFCC primary reference procedures for the measurement of catalytic activity concentrations of enzymes at 37 degrees C. International Federation of Clinical Chemistry and Laboratory Medicine. Part 7. Certification of four reference materials for the determination of the enzymatic activity of gamma-glutamyltransferase, lactate dehydrogenase, alanine aminotransferase and creatine kinase accord. Clin Chem Lab Med. 2002;40(7):739-745.
 43. Greaves M, Maley CC. Clonal evolution in cancer. Nature. 2012;481(7381):306–313.
 44. Kabel AM, Abdel-Rahman MN, El-Sisi Ael-D, Haleem MS, Ezzat NM, El Rashidy MA. Effect of atorvastatin and methotrexate on solid Ehrlich tumor. Eur J Pharmacol. 2013; 713(1-3):47-53.
 45. Gupta I, Burney I, Al-Moundhri MS, Tamimi Y. Molecular genetics complexity impeding research progress in breast and ovarian cancers. Mol Clin Onc. 2017;7(1):3-14.
 46. Bianchi-Frias D, Damodarasamy M, Hernandez SA, Gil da Costa RM, Vakar Lopez F, Coleman I, Reed MJ, Nelson PS. The aged microenvironment influences the tumorigenic potential of malignant prostate epithelial cells. Molecular Cancer Research. 2019;17(1):321-331.
 47. El-Masry TA, Al-Shaalan NH, Tousson E, Buabeid M, Alyousef AM. The therapeutic and antineoplastic effects of vitamin B17 against the growth of solid-form Ehrlich tumours and the associated changes in oxidative stress, DNA damage, apoptosis and proliferation in mice. Pak. J. Pharm. Sci. 2019;32(6):2801-2810.
 48. Mutar TF, Gazia MA, Salem SB, Hammed EH, Tousson E. Ehrlich ascites carcinoma bearing mice as model of human hepatocellular carcinoma. Asian Journal of Research and Reports in Hepatology. 2019;1(1):1-9.
 49. Tousson E, Hafez E, Gazia MMA, Salem SB, Mutar TF. Hepatic ameliorative role of vitamin b17 against ehrlich ascites carcinoma–induced liver toxicity. Environmental Science and Pollution Research. 2020;27(9):9236-9246.
 50. Zhang S, Gao H, Bao G. Physical Principles of Nanoparticle Cellular Endocytosis. ACS Nano. 2015;9(9):8655–8671.
 51. Zhang S, Li J, Lykotrafitis G, Bao G, Suresh S. Size-dependent endocytosis of nanoparticles. Adv. Mater. 2009;21(4):419–424.
 52. Aguzzi C, et al. Chitosan-silicate biocomposites to be used in modified drug release of 5-aminosalicylic acid (5-ASA). Appl. Clay Sci. 2010;50(1):106–111.
 53. Alkhatib MH, Alkreathy HM, Balamash KS, Abdu F. Antitumor activity of doxorubicine-loaded nanoemulsion against Ehrlich ascites carcinoma-bearing mice. Tropical Journal of Pharmaceutical Research. 2016; 15(5):937-943.
 54. Maliver P, Festag M, Bennecke M, Christen F, Bánfai B, Lenz B, Winter M. Assessment of Preclinical Liver and Skeletal Muscle Biomarkers Following Clofibrate Administration in Wistar Rats. Toxicol Pathol. 2017;45(4):506-525.
 55. Brancaccio P, Lippi G, Maffulli N. Biochemical markers of muscular damage. Clinical Chemistry and Laboratory Medicine. 2010;48(6):757-767.
 56. Shin KA, Park KD, Ahn J, Park Y, Kim YJ. Comparison of changes in biochemical markers for skeletal muscles, hepatic metabolism, and renal function after three types of long-distance running: observational study. [J] Medicine. 2016; 95(20):1-6.
 57. Moghadam-Kia S, Oddis CV, Aggarwal R. Approach to asymptomatic creatine kinase elevation. Cleveland Clinic Journal of Medicine. 2016;83(1):37-42.
 58. Lee EM, Kim DY, Kim AY, et al. Chronic effects of losartan on the muscles and the serologic profiles of mdx mice. Life Sciences. 2015;143:35–42.
 59. Veropalumbo C, Giudice E, Esposito G, Maddaluno S, Ruggiero L, Vajro P. Aminotransferases and muscular diseases: a disregarded lesson. Case reports and review of the literature. Journal of Paediatrics and Child Health. 2012;48(10): 886-890.
 60. Mcmillan HJ, Gregas M, Darras BT, Kang PB. Serum transaminase levels in boys with Duchenne and Becker muscular dystrophy. Pediatrics. 2011;127(1):132-136.
 61. Wang Y, Yang F, Zhang HX, et al. Cuprous oxide nanoparticles inhibit the growth and metastasis of melanoma by targeting

- mitochondria. *Cell Death Dis.* 2013;4(8): e783. 1-10.
62. Lord MS, Tsoi B, Gunawan C, Teoh WY, Amal R, Whitelock JM. Anti-angiogenic activity of heparin functionalised cerium oxide nanoparticles. *Biomaterials.* 2013; 34(34):8808–8818.
63. Dahle JT, Livi, K, Arai Y. Effects of pH and phosphate on CeO₂ nano-particle dissolution. *Chemosphere. Epub.* 2015; 119:1365-1371.
64. Papakostidi A, Tolia M, Tsoukalas N. Quality assurance in Health Services: the paradigm of radiotherapy. *J BUON.* 2014;19(1):47–52.
65. Sveistrup J, Rosenschöld PM, Deasy JO, et al. Improvement in toxicity in high risk prostate cancer patients treated with image-guided intensity-modulated radiotherapy compared to 3D conformal radiotherapy without daily image guidance. *Radiat Oncol.* 2014;9:44: 1-8.
66. Abd El-Aziz AF, Hefni ME, Shalaby AM. Inhibitory effects of Rosemary (*Rosmarinus officinalis* L.) on Ehrlich ascites carcinoma in mice. *International Journal of Current Research Academic Review.* 2014;2(9): 330–357.
67. Moselhi SS, Al Mslmani MB. Chemopreventive effect of lycopene alone or with melatonin against the genesis of oxidative stress and mammary tumors induced by 7,12 dimethyl(a) benzanthracene in sprague dawely female rats. *Molecular and Cellular Biochemistry.* 2008;319(1-2):175-180.
68. Abd El-Dayem SM, Fouda F, Helal M, Zaazaa A. The role of Catechin against doxorubicin-induced cardiotoxicity in Ehrlich ascites carcinoma cells (EAC) bearing mice. *American Journal of Science.* 2010;6(4):146–152.
69. Bjelland S, Seeberg E. Mutagenicity, toxicity and repair of DNA base damage induced by oxidation. *Mutat. Res.* 2003; 531(1-2):37–80.
70. El-Moselhy KM, Othman AI, El-Azem HA, El-Metwally MEA. Bioaccumulation of heavy metals in some tissues of fish in the Red Sea, Egypt. *J. Basic Appl. Sci.* 2014;1: 97–105.
71. Navarro J, Obrador E, Carretero J, Petschen I, Avino J, Perez P, Estrela JM. Changes in glutathione status and the antioxidant system in blood and in cancer cells associate with tumour growth in vivo. *Free Radic. Biol. Med.* 1999;26(3-4):410–418.

© 2021 AL-Ahmari and El-Hamidy; This is an Open Access article distributed under the terms of the Creative Commons Attribution License (<http://creativecommons.org/licenses/by/4.0>), which permits unrestricted use, distribution, and reproduction in any medium, provided the original work is properly cited.

Peer-review history:
The peer review history for this paper can be accessed here:
<http://www.sdiarticle4.com/review-history/67301>